PLANE STRAIN CRACK TOUGHNESS OF FIBERGLASS REINFORCED PLASTIC

BY

THOMAS HARRY AULENBACH
LIEUTENANT, UNITED STATES NAVY
B.S., UNITED STATES NAVAL ACADEMY
(1963)

SUBMITTED IN PARTIAL FULFILLMENT
OF THE REQUIREMENTS FOR THE DEGREE OF
NAVAL ENGINEER
AND THE DEGREE OF
MASTER OF SCIENCE IN MECHANICAL ENGINEERING
AT THE
MASSACHUSETTS INSTITUTE OF TECHNOLOGY
MAY, 1969

ABSTRACT

PLANE STRAIN CRACK TOUGHNESS OF FIBERGLASS REINFORCED PLASTIC

by

THOMAS HARRY AULENBACH

Submitted to the Departments of Naval Architecture and Marine Engineering and of Mechanical Engineering on May 23, 1969, in partial fulfillment of the requirements for the Master of Science degree in Mechanical Engineering and the Professional Degree, Naval Engineer.

The plane strain crack toughness K_{1c} is a material property which is measured in terms of the opening mode stress intensity factor K_{1c}, expressed in units of (stress) x (length)$^{\frac{1}{2}}$. The recommended specimen design of four point bend samples for plane strain crack toughness testing of high strength metallic materials is compared with results of tests using fiberglass reinforced plastics (FRP). This comparison indicates that the rules and guidelines used for testing metals do not apply to FRP. The variation of K_{1c} with specimen thickness, notch depth, glass content and strain rate are presented in tabular and graphical form.

Recently many authors have reported increases of up to an order of magnitude in the fracture surface work of epoxy and polyester resins when an elastomeric second phase is added to the unreinforced matrix. The results of test using CTBN rubber modified LAMINAC 4173 reinforced with Style 181 fiberglass fabric are reported. The surface work increased by only a factor of two for the composite system used. These results indicate that toughening the matrix does not necessarily toughen the composite.

THESIS SUPERVISOR: F.J. MCGARRY

TITLE: PROFESSOR, DEPARTMENT OF CIVIL ENGINEERING

ACKNOWLEDGMENT

I would like to express my sincere appreciation to Professor F.J. McGarry, Department of Civil Engineering, Massachsuetts Institute of Technology, for his advice, guidance, criticism and encouragement. Without his aid and assistance this thesis would not have been possible.

The assistance of Mr. James King and Mr. Arthur Rudolph was invaluable to the author for technical advice and helpful suggestions for the cutting and machining of the specimens. Several graduate students, research assistants and teaching assistants offered background and technical information, helpful comments and useful criticism. Their contributions are hereby acknowledged.

TABLE OF CONTENTS

LIST OF SYMBOLS

A_n = n^{th} polynomial coefficient

a = Crack length

B = Thickness of bend specimen

E = Young's Modulus

ΔE = Change in Young's Modulus with the addition of CTBN rubber

G = Strain energy release rate

G_{1c} = Critical opening mode strain energy release rate

g_o = Distance between gage points

K_1 = Opening mode stress intensity factor

K_{1c} = Critical opening mode stress intensity factor

ΔK_{1c} = Change in K_{1c} with the addition of CTBN rubber

l = Specimen length

M = Applied bending moment

P = Applied force

V = Change in length of LVDT

w = Specimen width

X = Displacement coefficient, EVB/P

Y = Dimensionless stress intensity factor

γ = Fracture surface work

σ = Applied stress

σ_{ys} = Yield stress (also numerically equal to ultimate tensile stress for the fiberglass reinforced plastics tested)

LIST OF FIGURES

LIST OF TABLES

INTRODUCTION

Recent technological advances in structural materials have indicated the potential of filament reinforced composites for providing greater structural efficiency than high strength metals. Composite materials can be tailored to the design situation giving such desirable characteristics as high strength-to-weight ratio, excellent resistance to corrosion, ease of maintenance, and, generally, are formable into any shape without the need for extremely heavy equipment as is required for the shaping of most high strength metals. However, before composites can be used to the fullest extent, there are several engineering problems which must be solved. When thermosetting polymer matrices are employed, their usefulness is seriously limited by their brittleness and susceptibility to crack initiation and propagation. Materials which fail without warning after undergoing negligible plastic flow and which are extremely sensitive to the presence of flaws acting as stress concentrators are limited in usefulness to stress levels significantly lower than their ultimate tensile stress.

Fracture toughness testing of fibrous composites is in its infancy. Although a great deal has been done with brittle metals (1,2),* it is questionable if the practices

---

* The numbers refer to the List of References.

and guidelines developed for metals can be used when testing composites. The purpose of this investigation is therefore threefold:

1) To test the applicability of present testing procedures for fracture toughness testing of metallic materials as stated in Reference 1 when applied to fiber reinforced plastics.

2) To test the variation of fracture toughness with thickness and glass-to-resin ratio.

3) To investigate the effect on fracture toughness by the addition of an elastomeric second phase such as CTBN rubber.

The plane strain crack toughness, K_{1c}, is a material property which is measured in terms of the opening-mode stress intensity factor K_1, expressed in units of (stress) x $(\text{length})^{\frac{1}{2}}$. To determine a K_{1c} value, a crack-notched specimen is increasingly loaded until the crack becomes unstable and extends abruptly. The ratio of K_1 to the applied load is a function of specimen design and the value of K_1 corresponding to the load at which unstable crack extension is observed is the K_{1c} value determined by the test. It is necessary to develop specifications for valid K_{1c} testing for fiberglass reinforced plastics as was reported in (1) for high strength metals.

The second phase of this report deals with the variation in K_{1c} with the number of layers of cloth and with

the glass-to-resin ratio. The purpose here is to optimize the number of layers and the glass-to-resin ratio in order to provide a material with the best possible crack toughness.

The final phase evaluates the addition of an elastomeric second phase to the resin which is intended to enhance the toughness of the composite. Recently, many authors (3,4, 5) have reported significant toughening of polyester and epoxy resins when certain types of elastomers are added. The purpose here is to determine the effect of adding CTBN rubber to the resin and discover if toughening the resin necessarily toughens the composite.

MATERIALS

The fiberglass reinforced plastic (FRP) specimens used in this report were constructed of Laminac 4173 polyester resin, supplied by American Cyanamid Company, and reinforced with Stevens Style 181 fiberglass fabric. Methyl ethyl ketone peroxide (MEKP) was used as the hardening agent. The elastomeric second phase which was added to the resin for part 3 of this report was CTBN rubber manufactured by the B.F. Goodrich Chemical Company.

Laminates were constructed using the standard vacuum bag technique (see Appendix I) and cured in the hydraulic press available in the Department of Civil Engineering, Massachusetts Institute of Technology. The laminates were subjected to a pressure of 120 psi and cured in the press at a temperature of 200°F for one hour. After removal from the press, the laminates were post cured in an electric oven for two hours at a temperature of 250°F. The numbers of layers varied from a minimum of the 3 to a maximum of 48. Standard tensile specimens and four point bend specimens were then cut (see Figure 1) and tested in an Instron Universal Testing Machine.

METHOD OF INVESTIGATION

The types and basic principles of instrumentation suitable for detecting crack extension in fracture toughness tests have been reported in (7). For plane strain toughness testing, these methods include measurement of displacement, electrical potential, acoustic emission and ink staining. For the purposes of this report it was felt that measurement of the displacement of points symmetrically located from the crack would give accurate results and the equipment required to employ this technique was readily available. A linear variable differential transformer (LVDT) with a displacement constant of 0.002 inches of deflection per inch of Instron recording paper with a gage length of one inch was selected. Since the gage length was larger than the notch depth for most specimens tested, it was not possible to use existing calibration curves for converting displacement measurements to crack lengths.

The crack tip stress intensity factor K_1 in a test specimen is equal to the applied load multiplied by some function of the specimen dimensions. An established relation connecting K_1 with the specimen dimensions and the applied load for a particular specimen design is called a K-calibration.

The most commonly used experimental method of K-calibration is that due to Irwin and Kies (8) in which measurements are made of the compliance of a specimen having a narrow machined slot which is incrementally extended between successive

measurements. This procedure was followed to obtain an experimental displacement coefficient, S, as a function of a/w for an aluminum specimen of the same planar dimensions as those used for the purpose of this report. According to Irwin (8) the calibration specimen can be of any convenient material and aluminum was selected over fiberglass reinforced plastic for the following two reasons:

1. Aluminum is much easier to machine accurately

2. FRP has a tendency to be degraded appreciably with cyclical loading and it was feared that the repeated notching and testing would lead to erroneous results.

The displacement coefficient, X, $= \frac{EVB}{P}$

where E = Young's Modulus

V = Change in length of LVDT

B = Specimen Thickness

P = Applied load

Aluminum specimens, 7" by 1.5" by .125", were machine notched with a 1/32" cutter and tested in four point bending. The displacement of points symmetrically located from the notch were measured and recorded using the LVDT. To enhance the accuracy of the displacement coefficient calibration, ten identical specimens were tested with a/w between 0.10 and 0.60. The results are plotted in Figure 2.

Using Figure 2 it is possible to determine the depth of a notch in any material which is tested in four point bending and whose planar dimensions are in the ratio of 4:1.

All that is required is specimen dimensions and the slope of the load-deflection curve. Once a value of X has been determined, Figure 2 yields the value of a/w. This value of a/w will then be used to determine K via boundary collocation.

Boundary collocation K-calibration for single-edge cracked specimens in four point bending is reported by Gross and Srawley in (9). The K-calibration is represented by a fourth-degree polynomial of the following form to within 0.2% for all values of a/w up to 0.7:

$$K_1 = Y \frac{6Ma^{\frac{1}{2}}}{BW^2} \qquad \text{Equation 1}$$

Where $Y = A_o + A_1 (a/w) + A_2 (a/w)^2 + A_3 (a/w)^3 + A_4 (a/w)^4$

M = Applied bending moment

The coefficients A have the following values for four point bending with a ratio of length to width equal to four:

$$A_o = 1.99$$
$$A_1 = -23.19$$
$$A_2 = 12.97$$
$$A_3 = -23.19$$
$$A_4 = 24.80$$

Entering Figure 3 with the value of a/w obtained from the specimen dimensions, slope of the load deflection curve, and Figure 2 yields a value for Y. This is then used to calculate K_1 from equation 1.

EXPERIMENTAL METHOD

Laminates approximately 20" x 11" were prepared as outlined in Appendix A. The laminates were then cut into the following specimens: 4-four point bend beams 7" x 1.5", 5 standard ASTM tensile specimens and 3 double-edge-cracked specimens 8" x 3" which were used by Schulz (10) to investigate somewhat similiar effects using double-edge-cracked specimens.

The tensile tests were performed on an Instron Universal Testing Machine using a crosshead rate of 0.05 inches per minute. The longitudinal strain was determined with a PS-3M Wiedeman LVDT extensometer providing a direct recording of strain on the Instron chart paper. Tensile modulus and ultimate tensile strength were determined from the Instron load-displacement record.

Each of the four point bend specimens was milled parallel and then notched in the center using a cutter with a 45.0° included angle and a tip radius of 0.010 inches. The notch was then sharpened by tapping a single edge razor blade in the notch with a maul.

The specimens were then tested in four point bending using the LVDT to measure the displacement of points symmetrically located from the notch. The extensometer provided direct chart drive which yielded an accurate load-displacement curve from which the depth of the crack could be

determined as outlined previously. The parameters which were investigated include notch depth, thickness as controlled by the number of layers of fiberglass, crosshead speed, glass content, and percentage of CTBN rubber added.

Specimens of both 12 layers and 48 layers were notched to a depth varying from 0.135 to 0.900 inches. Two different thicknesses (12 layers and 48 layers) were used to determine if the notch depth effect is sensitive to thickness.

The crosshead speed was varied from 0.002 to 20.0 inches per minute using specimens with glass contents of approximately 42% and 70%. All of the specimens tested with 42% glass were cut from the same laminate whereas the 70% glass specimens were made from six different laminates with similar glass contents.

The number of layers of cloth varied from 3 to 48 layers of fiberglass fabric. Since the thin specimens had a tendency to buckle when subjected to four point bending, lateral support plates had to be used to insure that the specimens remained perpendicular to the testing jig and that buckling did not occur. The support plates had little effect on the final results except to introduce some additional friction. While the buckling and non-buckling cases are not identical, the plates were used in all cases in an attempt to minimize the relative effect of the plate friction whether or not buckling was anticipated.

To evaluate the effect of glass content, laminates of 18 layers of fiberglass were constructed with glass content varying from 41.5% to 83.6%. The amount of glass in each of the laminates was held constant and the quantity of resin used was varied. This was done because in most engineering applications the number of layers of cloth is determined by the maximum expected loads to be encountered in service.

Obtaining a glass content in excess of 85% is extremely difficult and requires a press with a high capacity. Also, the specimens with 83.6% glass tended to fail at the supports. This is due to the fact that there is not enough resin to transfer the load from one layer of cloth to the adjacent layer. At glass contents less than 40% there is considerable variation in the interstitial distances between adjacent layers of cloth. It was felt that had glass contents in the order of 20% been used erroneous results would have been obtained.

Four laminates with 15 layers of cloth were manufactured similar to the procedure outlined in Appendix A and using 2.5, 5.0, 7.5, and 10.0% of CTBN rubber. The percentages of rubber were based on the amount of resin used. The rubber is very viscous and it became necessary to heat the rubber up to a temperature of 150°F before it could be mixed with the resin. The mixture of rubber and resin was thoroughly stirred until a uniform index of refraction was evident. The MEKP

curing agent was added and the laminate was manufactured by the standard method. After the post curing, the laminate was cut into specimens as outlined previously and tested.

RESULTS

The results of the fracture toughness testing of four point bend specimens of LAMINAC 4173 polyester resin reinforced with Style 181 fiberglass cloth are presented. The effect of notch depth, specimen thickness, strain rate as controlled by the crosshead speed, the values of the material properties such as Young's Modulus and yield strength, and the variation in material properties which include K_{1c}, yield strength and Young's Modulus with different percentages of CTBN rubber added are reported. The effects of the different test variables are presented in the form of graphs and tables. The original tensile test data are reported in Table 2 for the unmodified resin and in Table 3 for the rubber modified resin.

The effect of notch depth is presented in Figure 4 and the data are presented as Table 4. For laminates with 48 layers of Style 181 fiberglass cloth the notch depth has no effect on K_{1c}. However, as can readily be seen in Figure 4, for laminates with 12 layers there is a considerable dependency of K_{1c} on notch depth.

Similar to high strength metals, fiberglass reinforced plastics exhibit a dependence of K_{1c} on specimen thickness. Figure 5 presents K_{1c} vs. thickness for specimens which contain approximately 70% glass by weight. The number of layers of cloth varied from a minimum of three to a maximum

of forty-eight. Figure 5a shows the dependence of $\left[\frac{K_{1c}}{\sigma_{ys}}\right]^2$ on thickness. The data are given in Table 5.

Strain rate can have a considerable effect on the results of the crack toughness tests. Figures 6 and 6a depict the effect of the Instron crosshead rate on K_{1c} and $[K_{1c}/\sigma_{ys}]^2$ respectively, for specimens which contain approximately 42 and 70% glass by weight. Note that in all cases the curves pass through a minimum in the region of 0.05 inches per minute. See Table 6 for the reduced test results.

As can be expected, there is a considerable variation in K_{1c} and $[K_{1c}/\sigma_{ys}]^2$ with glass content. Specimens were tested with from zero glass content to those with as high as 83.6% glass. Figures 7 and 7a show the effect of glass content on K_{1c} and $[K_{1c}/\sigma_{ys}]^2$ respectively. Note that as the glass content is increased, K_{1c} increases and the value of $[K_{1c}/\sigma_{ys}]^2$ passes through a minimum at about 70% glass (Table 7).

Specimens of 83.6% glass showed a strong tendency to either crush at the supports or fail in the compression region of the sample directly above the notch.

Yield strength of the fiberglass reinforced plastic tested followed the "rule of mixtures" almost exactly. Figure 8 is a plot of σ_{ys} vs. percent glass. The straight line on Figure 8 represents the locus of σ_{ys} vs. glass content assuming that the "rule of mixtures" applied. Young's Modulus, however, does not follow this rule and this can be seen from Figure 9.

Here, the curve plotted is the locus of E vs. glass content which resulted from the experimental data, not the "rule of mixtures". This data is presented as Table 8.

The effect of CTBN rubber added to the polyester resin is shown in Figures 10, 10a and 10b. Figure 10 shows the variation in both K_{1c} and $[K_{1c}/\sigma_{ys}]^2$ vs. percentage of CTBN rubber added. The value of K_{1c} and $[K_{1c}/\sigma_{ys}]^2$ passes through a peak at about 2.5% rubber. Both Young's Modulus and the yield strength also peaked at about 2.5% rubber. This test data is given as Table 9.

DISCUSSION OF RESULTS

The accuracy with which K_{1c} describes the fracture behavior depends upon how well the stress intensity factor represents the conditions of stress and strain inside the fracture process zone. An exact representation is only given by K_{1c} in the limit of zero plastic strain. For practical purposes, a sufficient degree of accuracy may be obtained if the crack front plastic zone is small in comparison with the vicinity around the crack in which the stress intensity factor yields a satisfactory approximation of the true stress field.

It has been suggested (1) that it is appropriate to assume that $[K_{1c}/\sigma_{ys}]^2$ is a characteristic dimension of the plastic zone which should be useful in estimating specimen dimensions to insure valid K_{1c} tests. The pertinent dimensions of four point bend specimens are notch depth and thickness. The assumption is that in order for a test to be valid both of these dimensions should exceed a certain multiple of $[K_{1c}/\sigma_{ys}]^2$

The effect of crack length on apparent K_{1c} is shown in Figure 4 for single-edge-cracked bend specimens of LAMINAC 4173 polyester resin reinforced with fiberglass. The specimens consisted of 12 and 48 layers. These correspond to thicknesses of 0.012" and 0.452" respectively (see Table 4). All of the specimens exhibited load-displacement curves with negligible nonlinearity after a minimum load was applied (there appeared to be a region where the curve was not linear

for low loads but it became a straight line after a few hundred pounds of force was applied). There was no trend or variation in K_{1c} with crack length for the samples which contained 48 layers of cloth. However, the 12 layer specimens displayed a dependency of K_{1c} on crack length, the shorter crack lengths indicated a higher value for K_{1c}. The average value of K_{1c} for all specimens except for the 12 layer samples with the smallest crack lengths was 23.1 $KSI \cdot (in)^{\frac{1}{2}}$ and this is considered to be the true value. While the data from these tests are limited, it does indicate that the apparent K_{1c} value increases for thin specimens with $a_o/[K_{1c}/\sigma_{ys}]^2$ ratios less then about 1.00. Reference (1) indicates that the value of $[K_{1c}/\sigma_{ys}]^2$ should be at least 2.5 for valid results when testing high strength metals. These test results indicate that there is an effect of thickness on the crack length chracteristic of FRP. More intermediate test results are necessary to set a lower limit on thickness to eliminate the effect of notch depth.

The influence of thickness is illustrated in Figure 5 and Figure 5a. The specimens contained from zero to 48 layers of cloth. The samples with no cloth were cast LAMINAC resin specimens 0.251" thick. All samples except the zero and three layer specimens contained approximately 70% glass. Figure 5 indicates that the results for specimens with less than 15 layers (0.123" thick) are invalid. No distinct "popin" occurred at thickness less then 0.073" (9 layers) and the results were difficult to analyze. This topic will be discussed more fully

later in this section. For all thicknesses greater than 15 layers (0.123"), complete fracture occurred at popin. These data (see Table 5) suggest that a ratio of $B/[K_{1c}/\sigma_{ys}]^2$ greater than 1.00 is necessary for valid K_{1c} determinations. For high strength metals, (1) indicates that this ratio should be at least 2.5.

It was anticipated that the strain rate and glass content would have a considerable effect on the results of crack toughness tests. This was born out by the test results as can be seen from Figure 6 and Figure 6a for strain rate and Figure 7 and Figure 7a for glass content. The test data are given in Table 6 and Table 7.

The "rule of mixtures" states that the yield stress of a composite (or any material property) is the sum of the component yield stress times the volume fraction of that component. In equation form, this reduces to the following for the materials used:

$$\sigma_{composite} = \sigma_{matrix}\, \nu_{matrix} + \sigma_{fiber}\, \nu_{fiber}$$

where V is the volume fraction.

Figure 8 indicates that the value of yield stress follows the rule of mixtures but Figure 9 shows that the modulus of elasticity does not. One-half of the modulus of elasticity of glass was used ($\frac{1}{2}$ of 10.0×10.0^6, or 5.0×10^6) and a fairly smooth, but not linear, curve resulted. The motivation for this approach is the fact that in a fabric only half of the

fibers are aligned in the load direction and, therefore, only half of the material carries any load.

The results of the addition of CTBN rubber to the resin are given in Figures 10, 10a and 10b for K_{1c} and $[K_{1c}/\sigma_{ys}]^2$ σ_{ys}, and E vs. percentage CTBN rubber added. The results of a similar series of tests conducted by Sultan and McGarry (3) agree with the results presented herein. The magnitude of the yield stresses in (3) are only one-half those reported here. This can be attributed to widely different glass contents between the two reports.

Reference (3) reports an increase in the surface work, σ, by a factor of eight for cleavages of specimens of three unreinforced rubber modified polyester resins. The results of the present experimental investigation do not agree with that result for one of the reinforced resins, LAMINAC 4173. For the reinforced resin, the value of both K_{1c} and $[K_{1c}/\sigma_{ys}]^2$ are only increased by a factor of approximately 1.5. The value of K_{1c} can be related to G_{1c}, the strain energy release rate, by

$$K_{1c} = [EG_{1c}]^{\frac{1}{2}} \qquad \text{Equation 2}$$

Since $G = 2\sigma$ Equation 2 can be rearranged to yield

$$\gamma = \frac{1}{2}\frac{K_{1c}^{2}}{E} \qquad \text{Equation 3}$$

Taking the derivative of Equation 3 and dividing by Equation 3 results in the following expression for the change in surface work with rubber modified fiberglass reinforced plastic:

$$\frac{\Delta\gamma}{\gamma} = \frac{\Delta[\frac{1}{2}\frac{K_{1c}^{2}}{E}]}{}$$

where

$$\Delta[\frac{1}{2}\frac{K_{1c}^{2}}{E}] = \frac{1}{2}\left[\frac{2E\ K_{1c}\Delta K_{1c} - K_{1c}^{2}\Delta E}{E^2}\right]$$

and finally

$$\frac{\Delta\gamma}{\gamma} = \frac{2\Delta K_{1c}}{K_{1c}} - \frac{\Delta E}{E}$$

The values of ΔK_{1c} and ΔE along with $\frac{\Delta\gamma}{\gamma}$ are given in Table 10. This results in a maximum value of $\frac{\Delta\gamma}{\gamma}$ of 0.825 for a rubber content of 2.5% CTBN.

One final general observation is worthy of note. In spite of the difficulties experienced when analyzing the load-displacement data for thin specimens it is reasonably certain that rapid or unstable crack propagation occurred. The first tests on thin specimens seemed to indicate that slow crack growth was occurring, but the load-deflection curve indicated a valid test. As soon as the crack started to grow the load became constant and the deflection increased fairly rapidly but not catastrophically. This seemed to indicate that the energy necessary to propagate the crack was being supplied by the Instron crosshead. A very simple test was

devised to determine whether the necessary energy was coming from the Instron or was being supplied by the release of strain energy. As soon as popin was indicated, the Instron crosshead was stopped. Every time that this was necessary, the crack continued to grow until the entire specimen had failed, revealing that the energy did, indeed, come from the release of strain energy.

CONCLUSIONS

On the basis of this investigation, the following conclusions appear to be valid:

1. The minimum specimen dimensions recommended for plane strain crack toughness testing of high strength metallic materials cannot be applied to fiberglass reinforced plastics. The high strength metallic recommendations are excessive by a factor of 2.5 for both the characteristic dimensions for four point bend specimens.

2. Valid plane strain crack toughness results can be obtained for fiberglass reinforced plastics using specimens 0.123 inches thick and having a glass content of 70% by weight. This corresponds to a 0.123 inch thick specimen with 15 layers of Style 181 fiberglass fabric.

3. The value of K_{1c} increases rapidly as the glass content is increased.

4. Addition of 2.5 pph CTBN rubber to LAMINAC 4173 polyester resin reinforced with Style 181 fiberglass cloth increases the value of K_{1c} and $[K_{1c}/\sigma_{ys}]^2$ by a factor of 1.5. Adding more than 2.5 pph CTBN rubber has a detrimental effect on K_{1c} and $[K_{1c}/\sigma_{ys}]^2$

5. Ultimate tensile stress and modulus of elasticity of LAMINAC 4173 polyester resin reinforced with Style 181 fiberglass fabric are increased by a factor of 1.5 when 2.5 pph

CTBN rubber is added. If the amount of CTBN is increased from 2.5 pph to 10.0 pph both ultimate tensile stress and modulus of elasticity are decreased.

6. When unreinforced LAMINAC 4173 is modified with 10.0 pph CTBN rubber the fracture surface work is increased by a factor of nine whereas the fracture surface work is less than doubled when 10.0 pph of CTBN is added to the reinforced resin.

7. The maximum degree of toughening is achieved when 2.5 pph CTBN rubber is added to the matrix of fiberglass reinforced plastics. The value of fracture surface work is nearly doubled.

REFERENCES

1. "Plane Strain Toughness Testing of High Strength Metallic Materials," ASTM Special Technical Publication No. 410, December 1966.

2. "Fracture Toughness Testing and Its Applications," ASTM Special Technical Publication No. 381, June 1964.

3. J.N. Sultan and F.J. McGarry, "Toughening Mechanisms in Polyester Resins and Composites," First Quarterly Progress Report, Contract AF 33(615)-2712, Materials Research Laboratory, Department of Civil Engineering, Massachusetts Institute of Technology, September 1965.

4. F.J. McGarry and A.M. Willner, "Toughening of an Epoxy Resin by an Elastomeric Second Phase," DSR 79545, Manufacturing Chemists' Association, March 1968.

5. K. Fletcher, R. Hayward and J. Mann, "Rubber Reinforced Polystyrene and Copolymers," Chemistry and Industry, 1965, pp. 1854-1863.

6. A.M. Willner and F.J. McGarry, "Crack Propagation Resistance of Rubber Modified Epoxy Resin," Third Quarterly Progress Report, Contract AF 33(615)2712, Materials research Laboratory, Department of Civil Engineering, Massachusetts Institute of Technology, March 1967.

7. J.E. Srawley and W.F. Brown, Jr., "Fracture Toughness Test Methods," Fracture Toughness Testing and Its Applications, ASTM STP 381 Am. Soc. Testing Mat., 1965, pp. 133.

8. G.R. Irwin and J.A. Kies, "Critical Energy Rate Analysis of Fracture Strength," Welding Journal Research Supplement, 33, 1954, pp. 193.

9. B. Gross and J.E. Srawley, "Stress Intensity Factors for Single-Edge-Notch Specimens in Bending or Combined Bending and Tension by Boundary Collocation of a Stress Function," Technical Note D-2603 NASA, January 1965.

10. W.J. Schulz, "Fracture Mechanics of Fibrous Composite," S.M. Thesis, Massachusetts Institute of Technology, Cambridge, Massachusetts, May 1969.

APPENDIX A

FABRICATION OF LAMINATES

The fiberglass reinforced plastic laminates were composed of LAMINAC 4173 polyester resin (American Cyanamid Company) reinforced with Style 181 woven glass fabric (J.P. Stevens Company). Methyl ethyl ketone peroxide was used as the catalyst. The laminates were layed up using a vacuum bag technique.

A vacuum bag was constructed from two pieces of mylar film which was cut approximately one and a half inches bigger than the glass cloth on three sides and about four inches bigger on the fourth side. The bottom piece of film was lined with two thicknesses of Mortite caulking cord. Small diameter rubber tubing was inserted along the inside edge of the caulking cord on the two sides that were perpendicular to the side with the four inch margin to facilitate movement of the entrapped air bubbles. Felt weather stripping was then placed along the inside edge of the tubing and on the inside edge of the caulking cord. Sufficient weather stripping was used to fill the margin on all four sides.

The resin was mixed using an amount of LAMINAC 4173 equal to the weight of cloth utilized in the laminate. Two percent by weight of methyl ethyl ketone peroxide was used as the catalyst and thoroughly mixed with the resin.

The bottom piece of mylar was coated with the resin mixture and three layers of cloth were applied. This procedure was repeated until the desired number of layers of cloth were used.

Steel spacers were used to control the thickness of the laminates of equal numbers of layers of cloth which, in turn, determines the percentage of glass in the final product. The thickness desired could be estimated by assuming that every three layers of fiberglass cloth contribute 1/32" to the final thickness for laminates which will have approximately 70% glass by weight. The spacers were placed in the vacuum bag just outside the four corners of the cloth. The easiest procedure was to cut a piece out of the weather stripping adjacent to each corner of the cloth and place the spacers in this position.

The remaining piece of mylar was then placed over the bottom and pressed onto the caulking cord to insure an air tight seal. A vacuum pump nipple was inserted in the top piece of mylar and the vacuum was attached. A suction was taken on the vacuum bag to remove all of the entrapped air. In order to remove air which had become entrapped in the resin and between the layers of cloth, a spatula was used on the vacuum bag to force these bubbles (which are readily seen since upon complete wetting of the cloth the laminate becomes transparent) into the felt lining. Once the bubbles are in the lining they migrate, under the action of the pump, to the nipple

and are removed. The purpose of the rubber tubing was to aid this migration and to help eliminate the air bubbles that remained in the felt from being squeezed back into the resin when the press made contact with the felt. In the case of thin laminates, contact with the felt could occur before the press made contact with the fiberglass and resin.

After all the air bubbles were removed, the vacuum bag arrangement is placed between two aluminum plates and inserted in the hydraulic press. Pressure is increased until firm contact is made between the aluminum plates and the spacers. The laminate is kept in the press under pressure (approximately 120 psi on the laminate, not on the hydraulic ram) for one hour at a temperature of 200°F. As soon as there was pressure on the laminate, the vacuum pump was disconnected and the nipple removed. This prevented the nipple from becoming clogged with the excess resin and permitted its reuse for additional laminates.

After one hour in the press the laminate was removed and placed in an oven at 250°F for two hours for post curing. For best results it is recommended that the laminate be post cured in the bag. It is then ready to cut into the desired specimens and tested.

Using this technique, laminates of any size and thickness can be produced limited only by the dimensions of the press. Thickness can be varied by using different sized spacers to give laminates with widely varying glass to resin ratios.

When using the Department of Civil Engineering of Massachusetts Institute of Technology's equipment, it should be noted that the pressure indicated on the installed gage represents the pressure on the ram which has an area of 49 square inches. This pressure can be converted to the pressure actually applied to the laminate by a conversion factor equal to the ratio of the ram area to the laminate area, that is $P_{ind.} \times (49/\text{area of laminate}) = P_{lam.}$

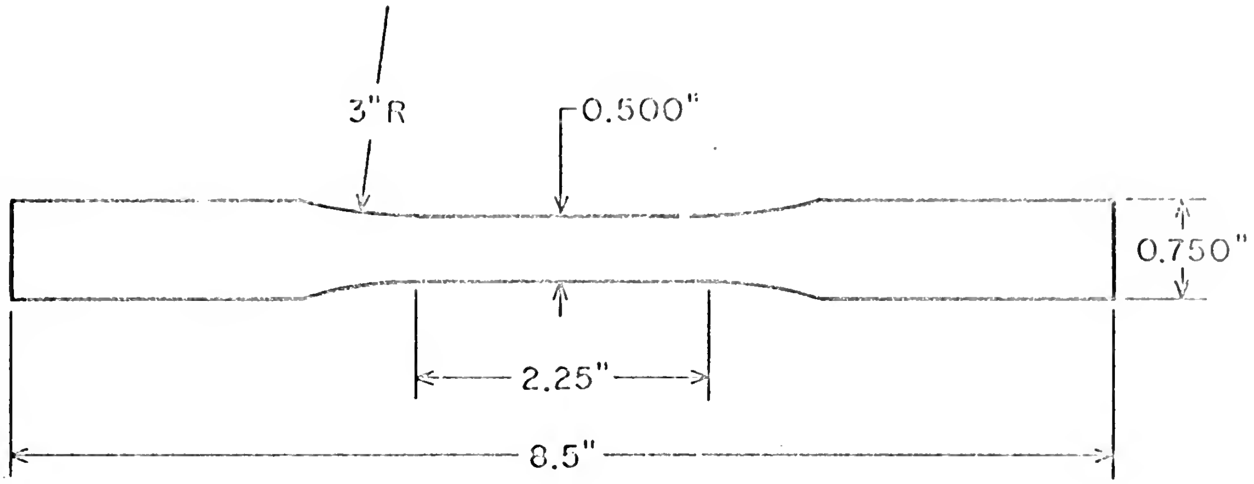

FIGURE 1. ASTM TENSILE TEST SPECIMEN D638 TYPE 1.

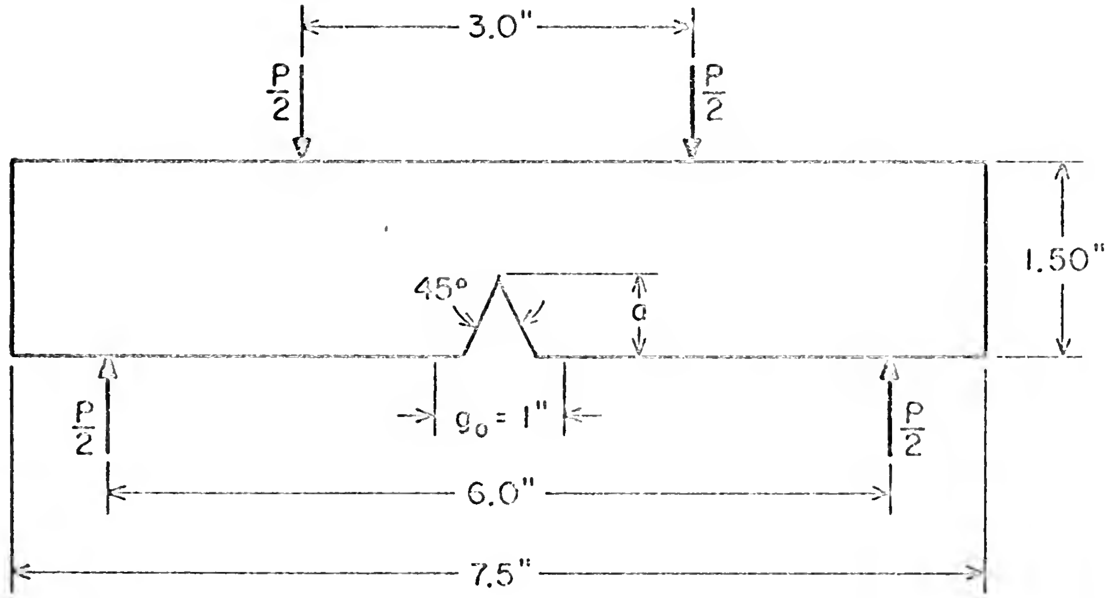

FIGURE 1a. FOUR POINT BEND SPECIMEN WITH LENGTH/WIDTH RATIO OF FOUR.

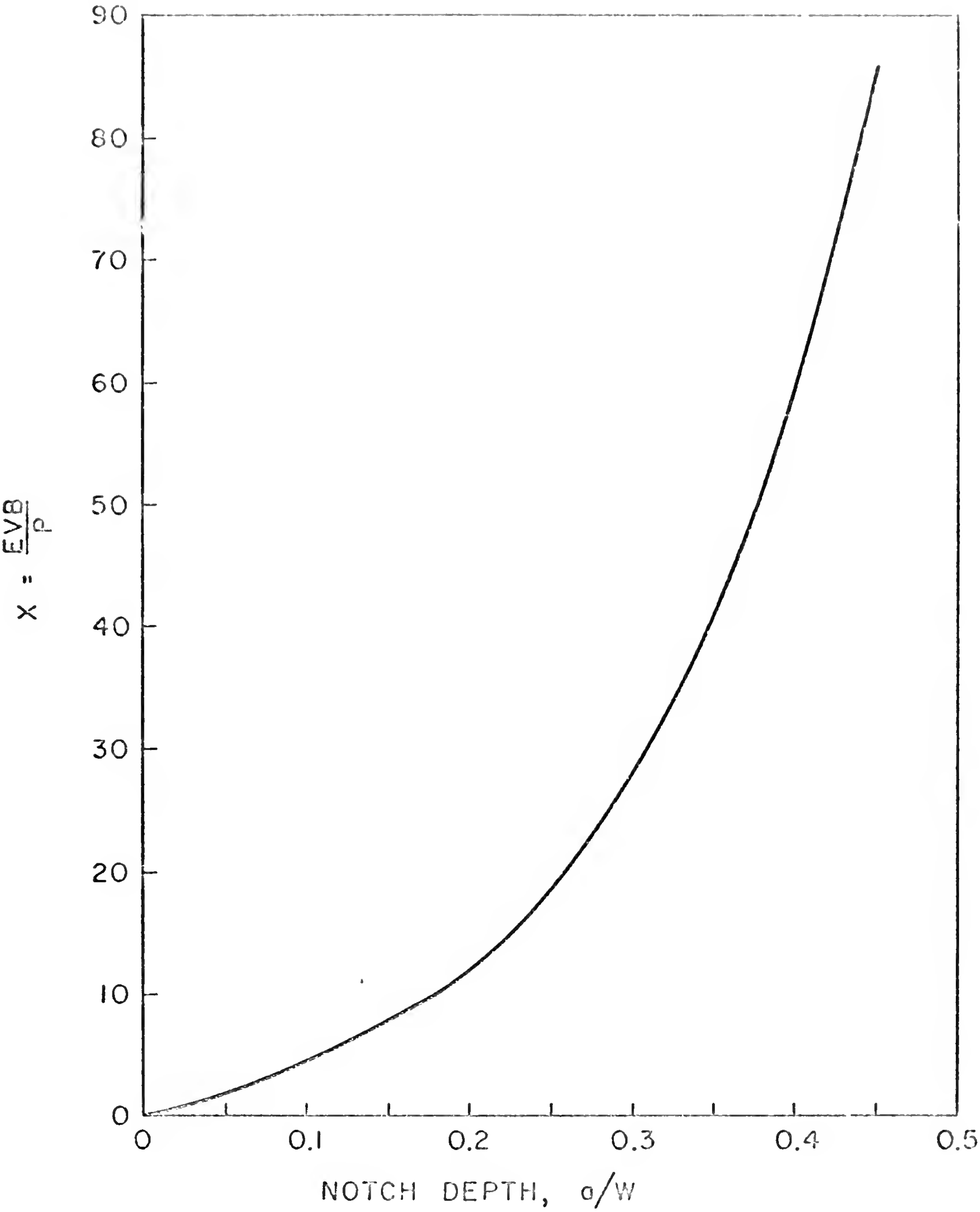

FIGURE 2. CALIBRATION CURVE FOR CONVERTING DISPLACEMENT MEASUREMENTS TO CRACK LENGTH FOR FOUR POINT BEND SPECIMENS.

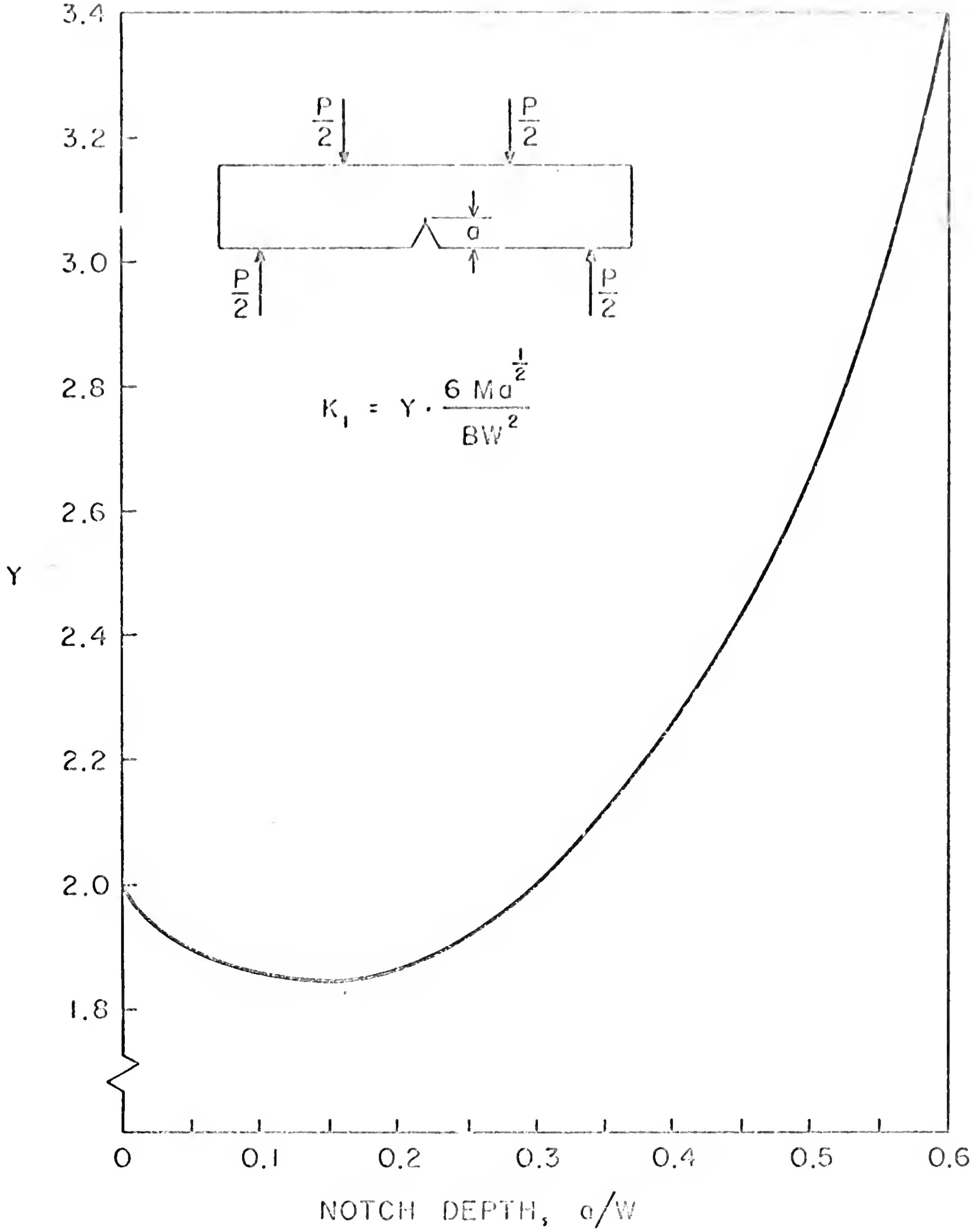

FIGURE 3. K CALIBRATION FOR FOUR POINT BEND SPECIMENS.

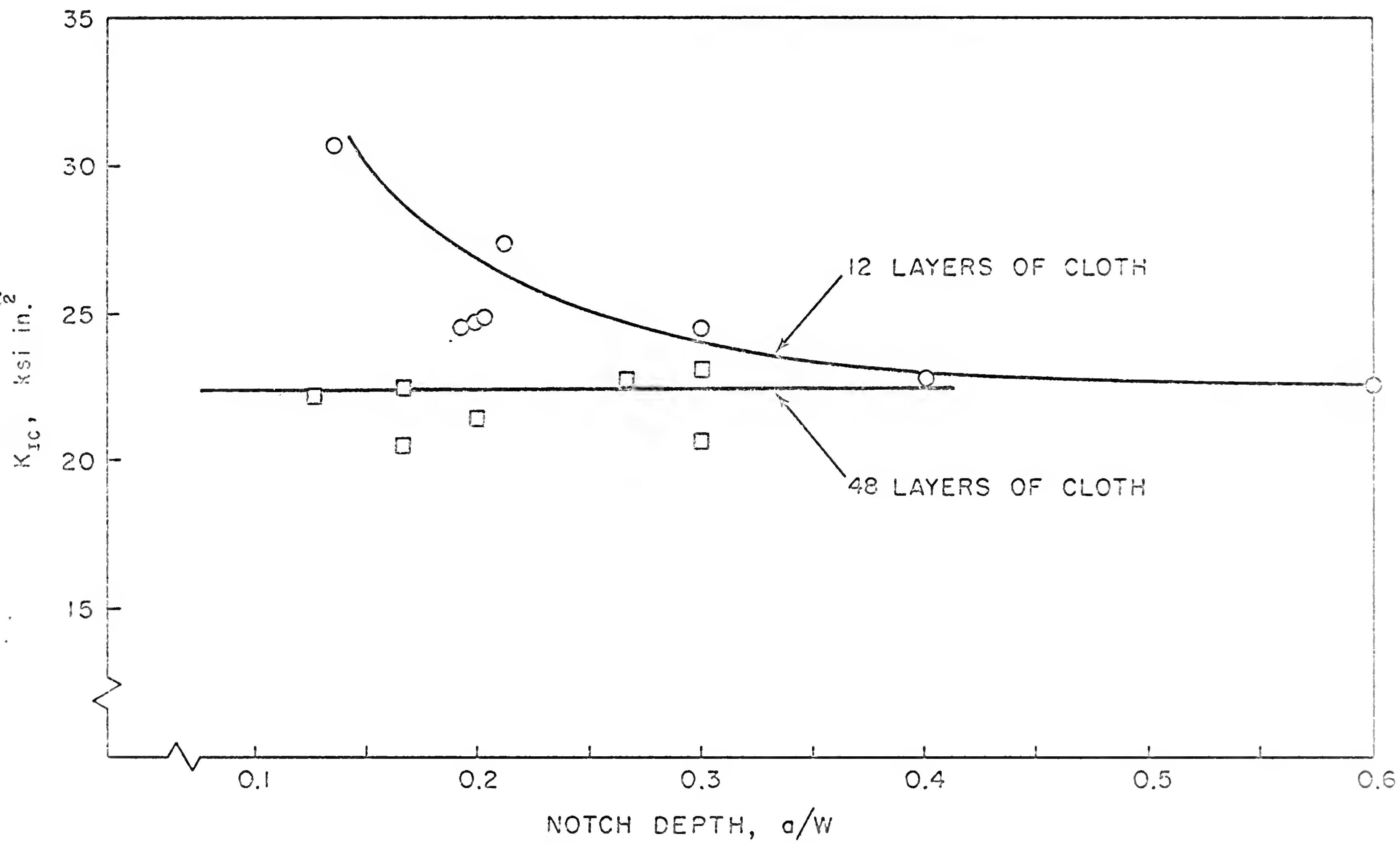

FIGURE 4. EFFECT OF NOTCH DEPTH ON APPARENT K_{IC}.

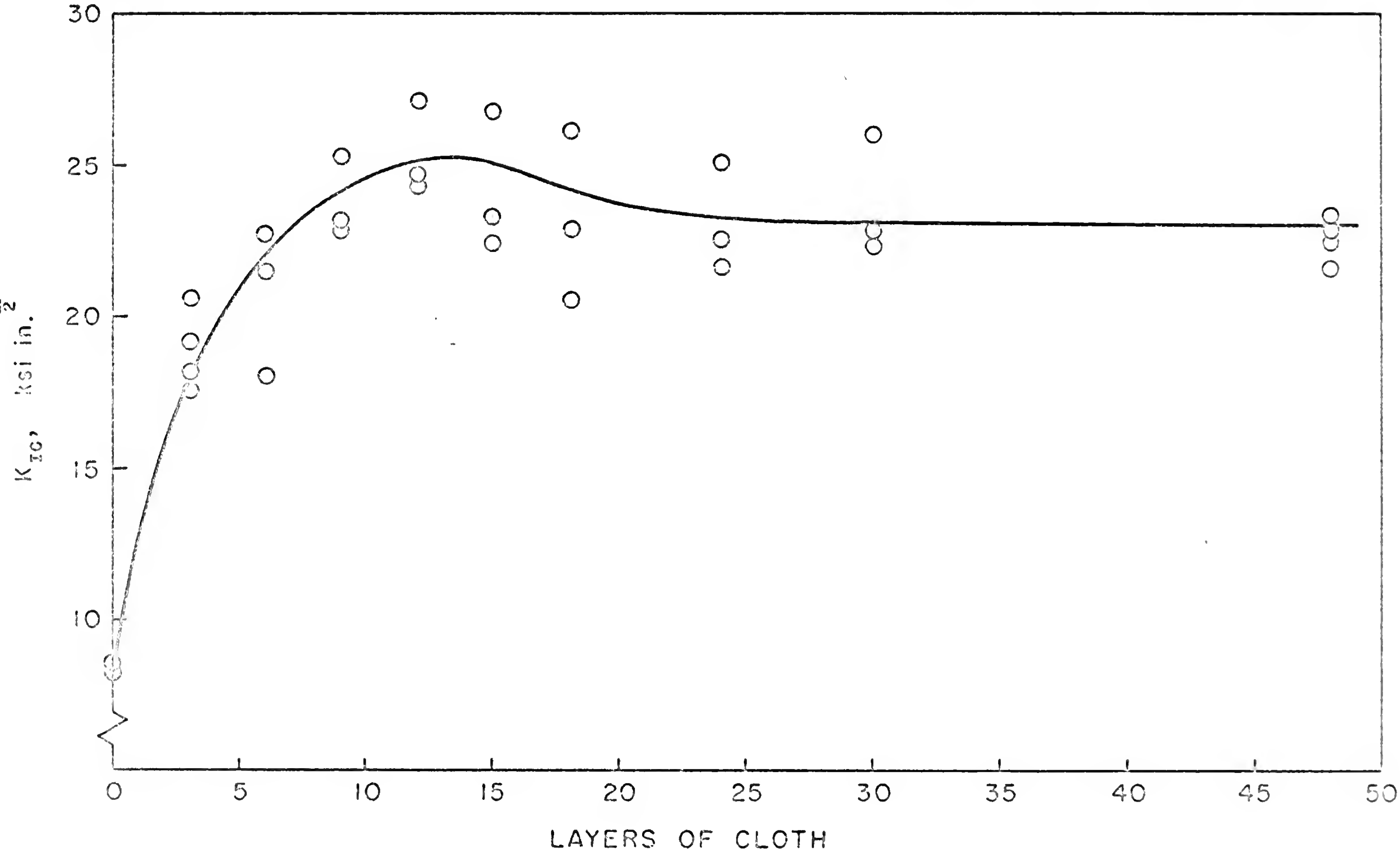

FIGURE 5. EFFECT OF NUMBER OF CLOTH LAYERS ON APPARENT K_{IC}.

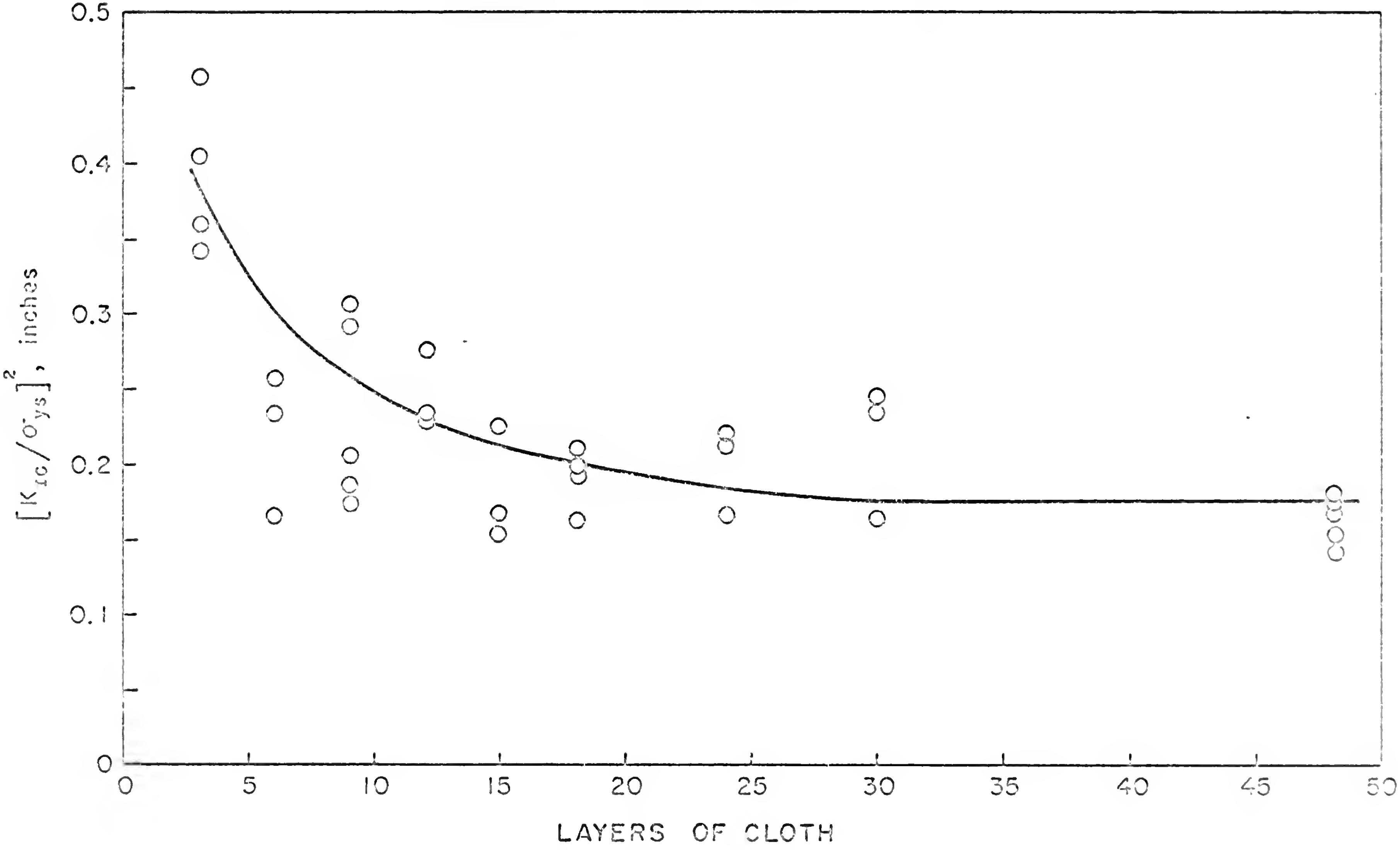

FIGURE 5a. EFFECT OF NUMBER OF CLOTH LAYERS ON $\left[K_{Ic}/\sigma_{ys}\right]^2$.

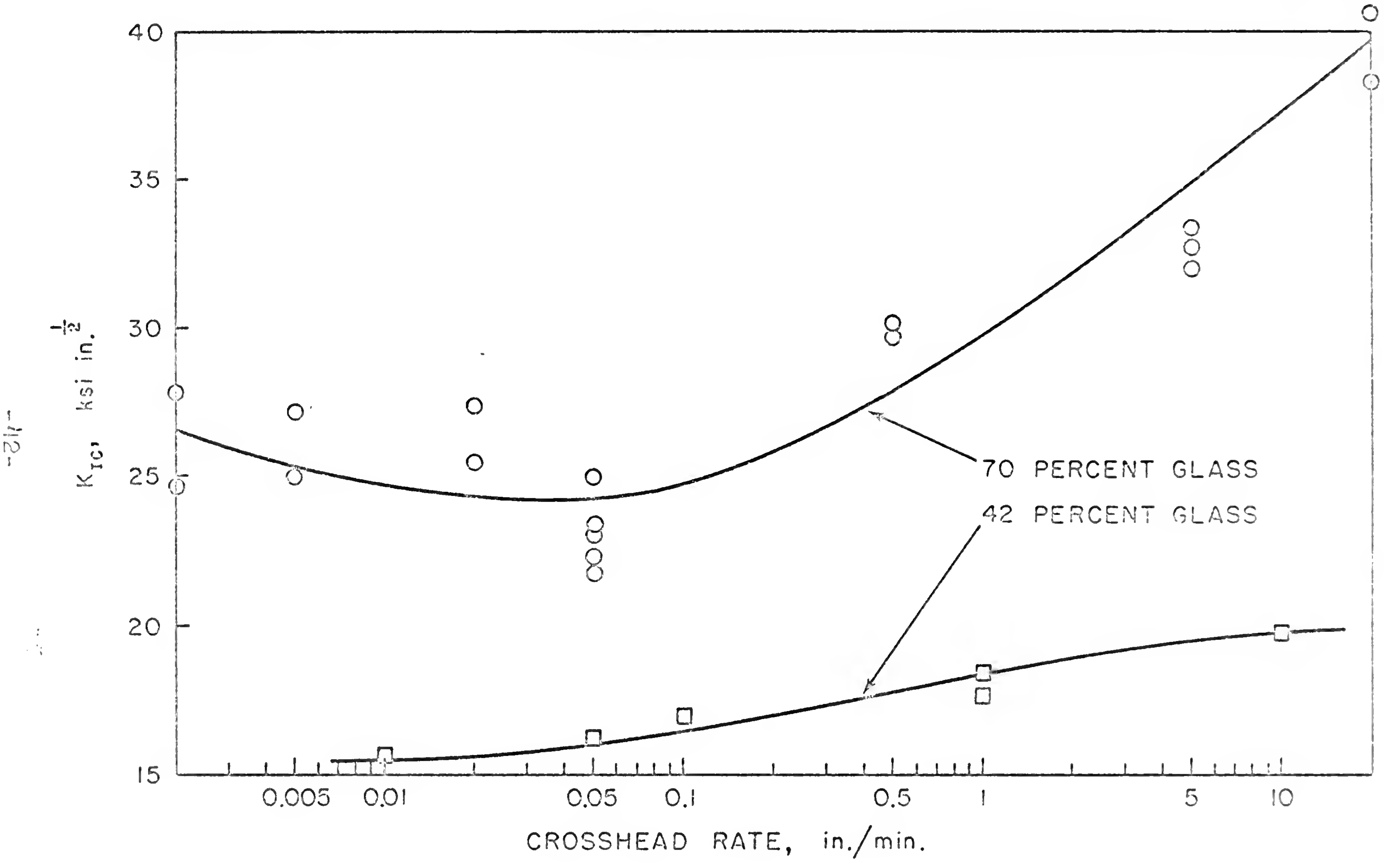

FIGURE 6. EFFECT OF CROSSHEAD RATE ON APPARENT K_{IC}.

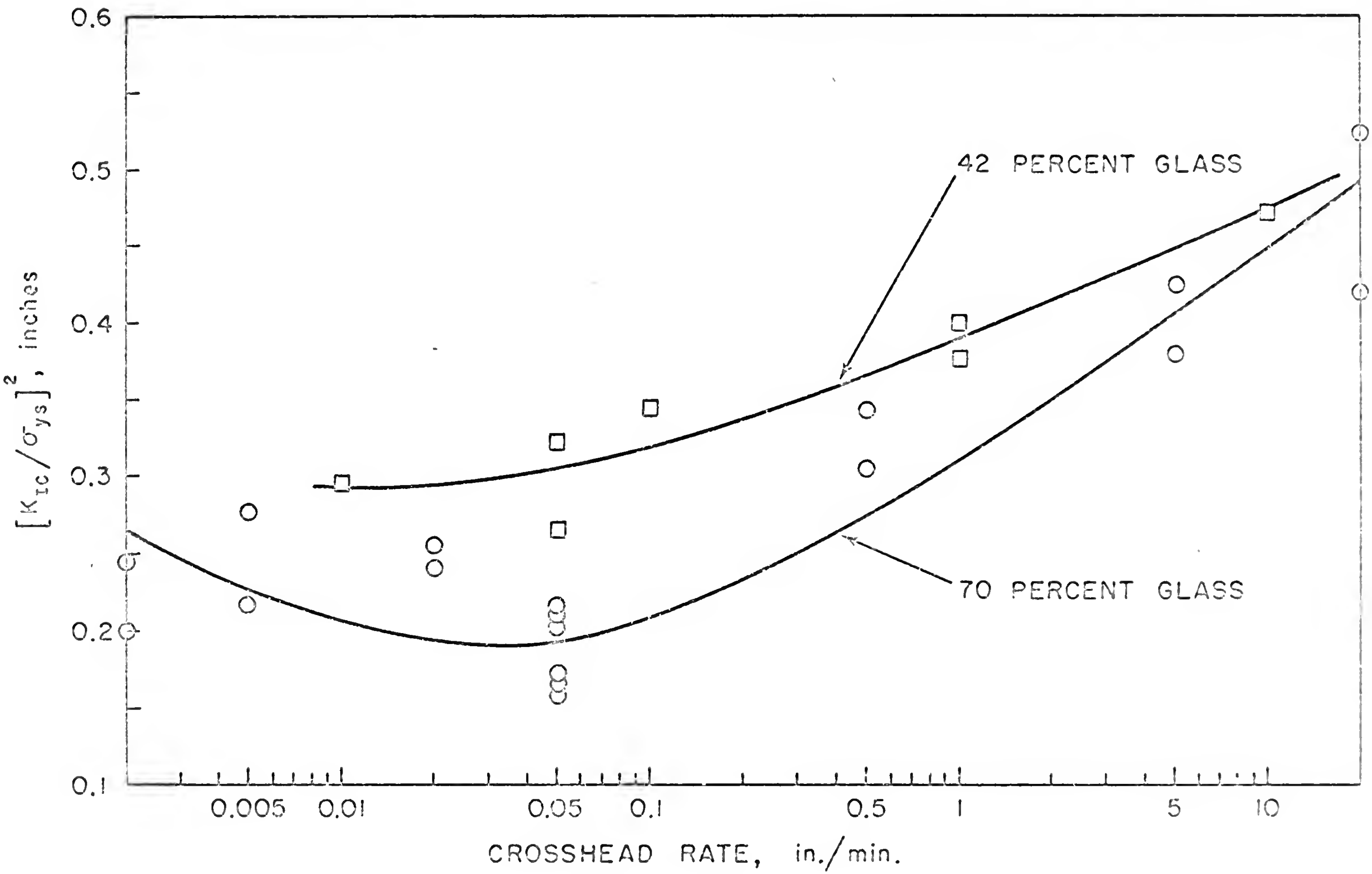

FIGURE 6a. EFFECT OF CROSSHEAD RATE ON $\left[K_{Ic}/\sigma_{ys}\right]^2$.

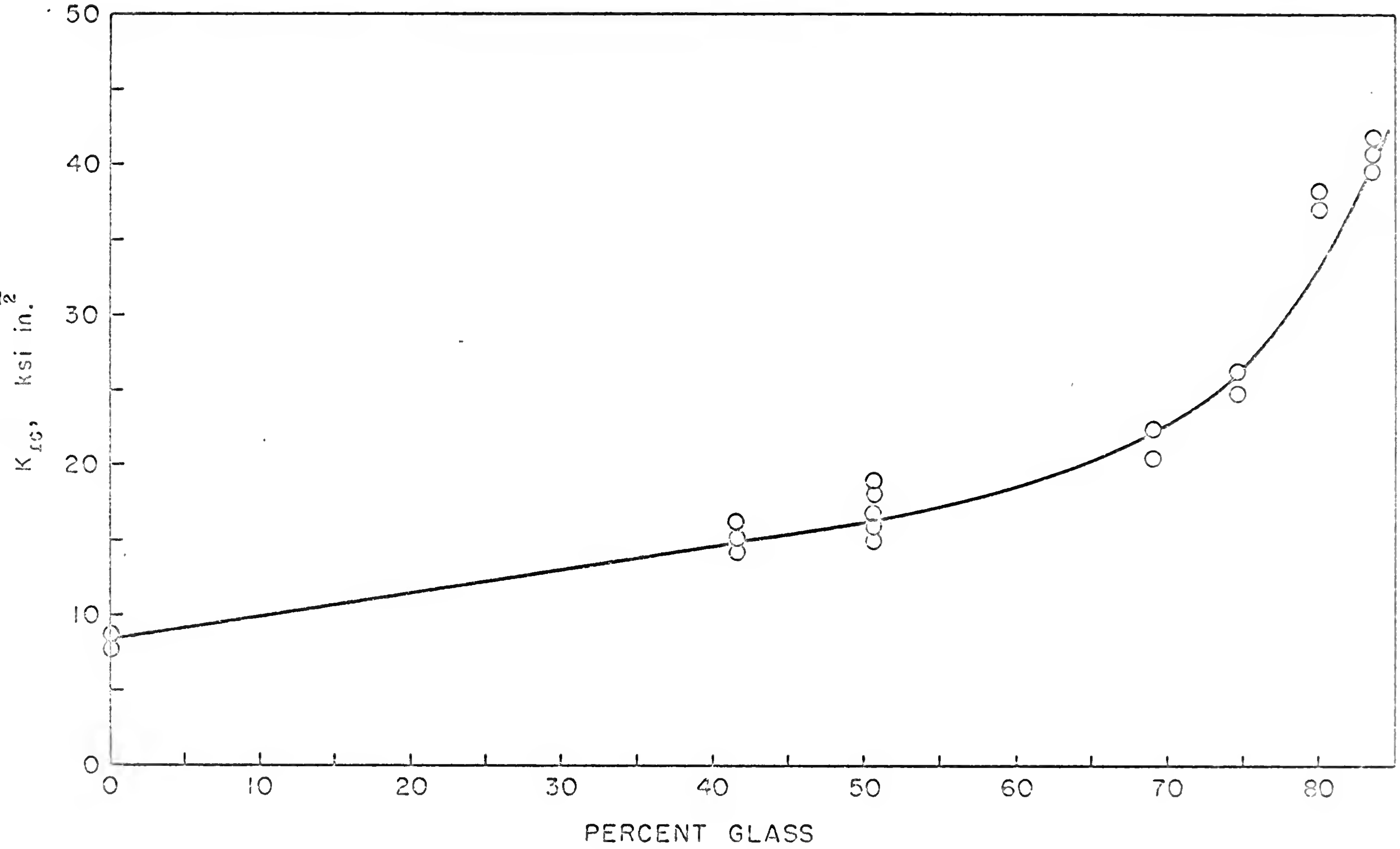

FIGURE 7. EFFECT OF GLASS CONTENT ON APPARENT K_{IC}.

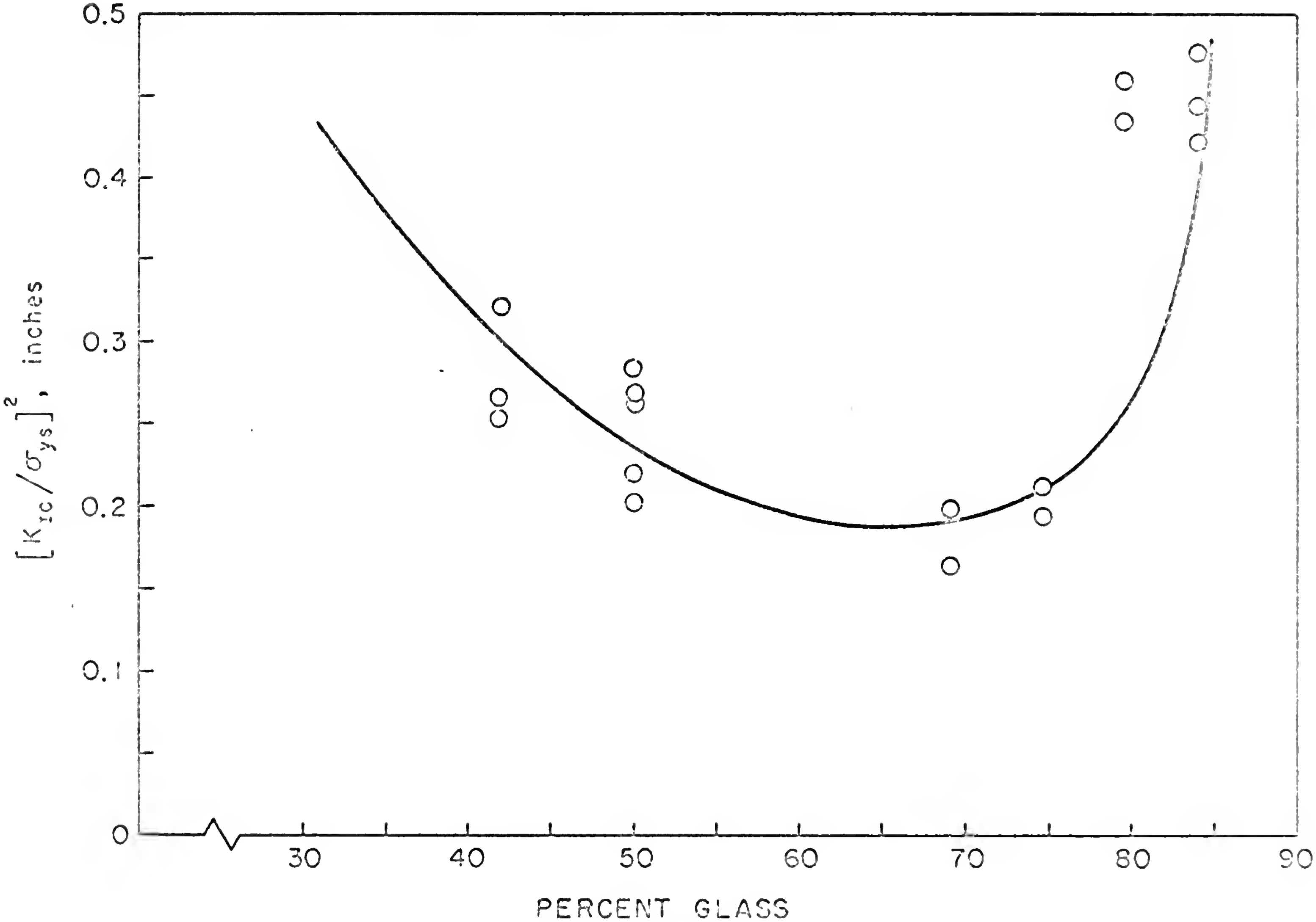

FIGURE 7a. EFFECT OF GLASS CONTENT ON $[K_{IC}/\sigma_{ys}]^2$.

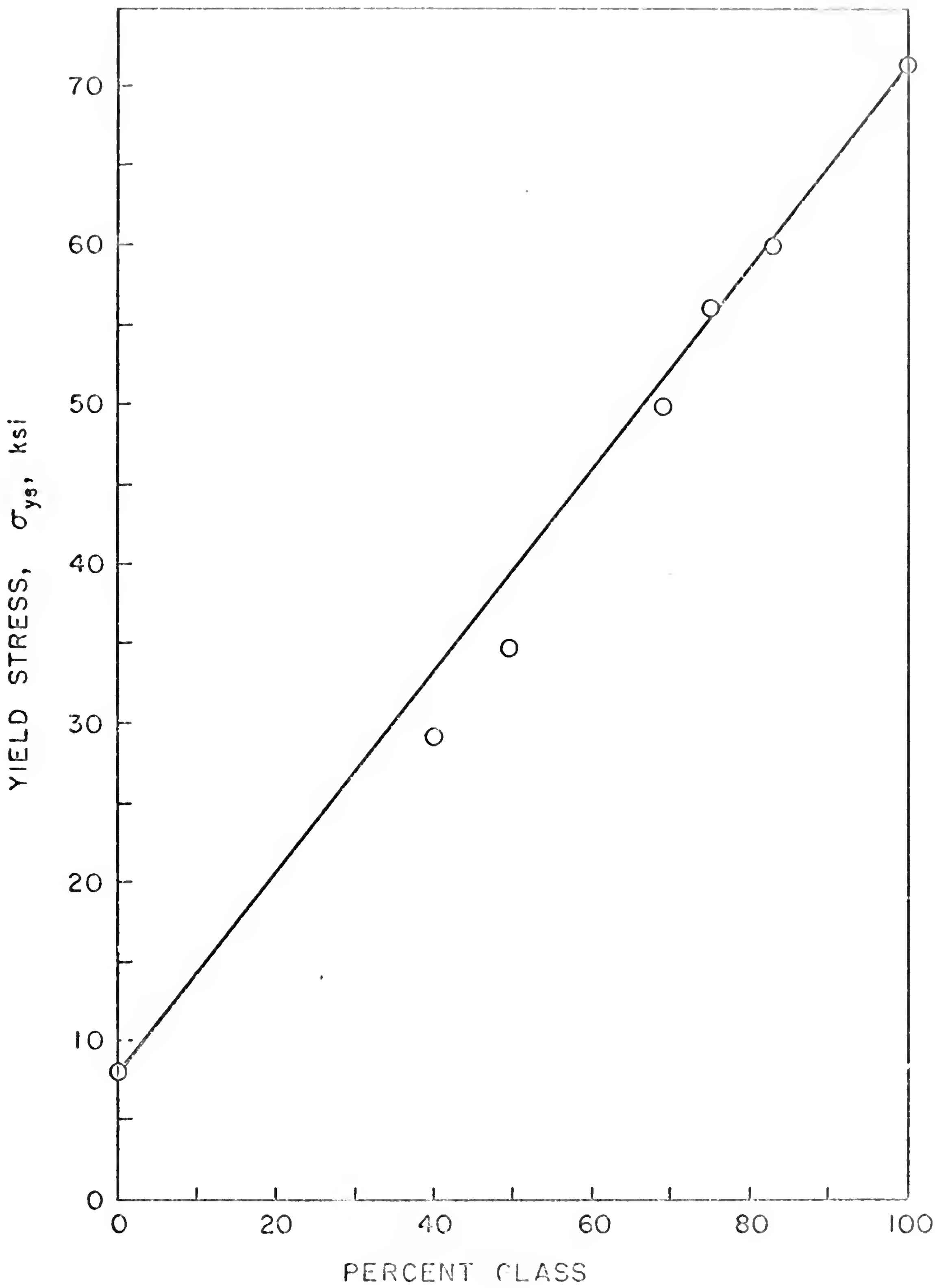

FIGURE 8. VARIATION IN YIELD STRESS WITH PERCENT GLASS BY WEIGHT.

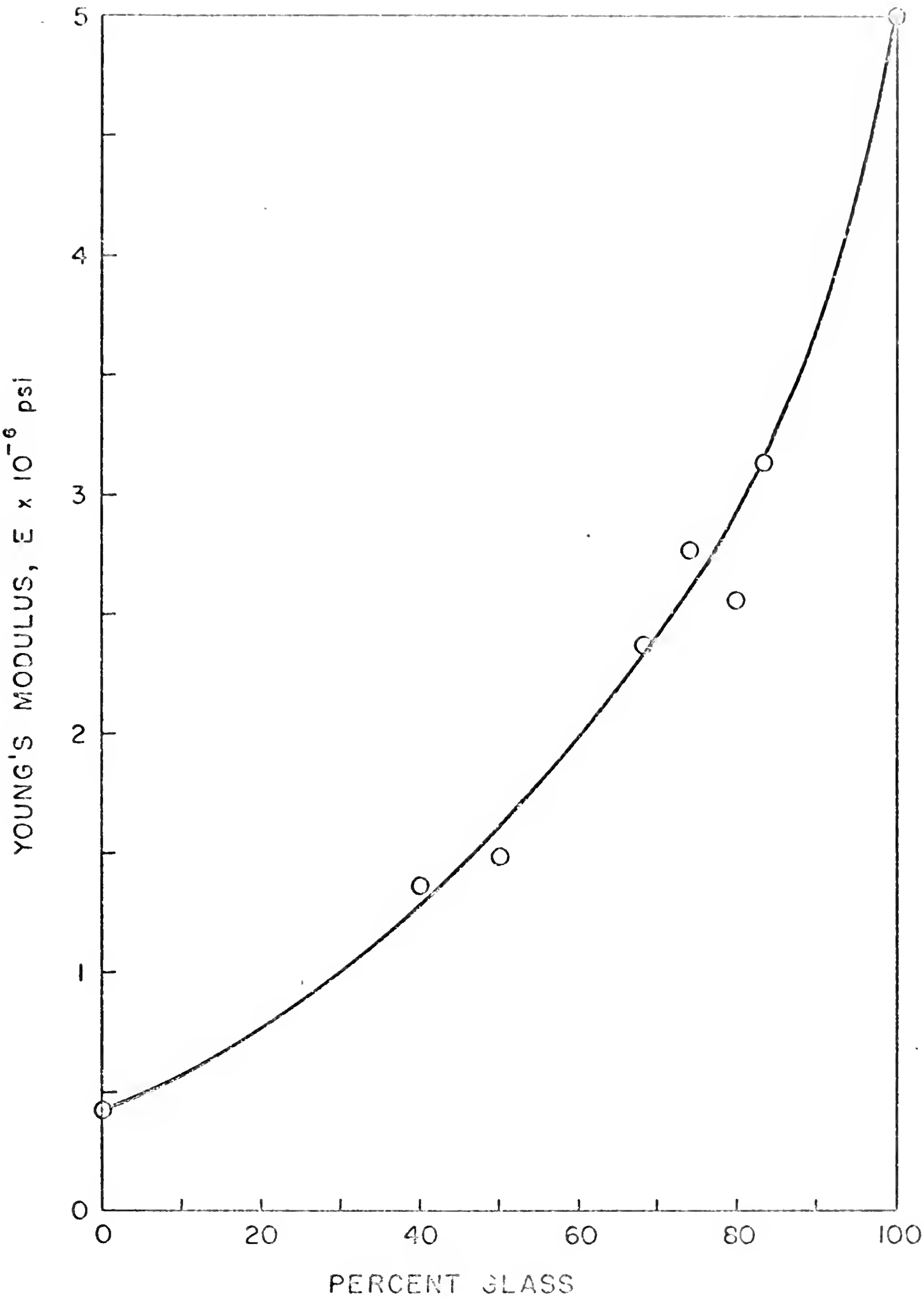

FIGURE 9. VARIATION IN YOUNG'S MODULUS WITH PERCENT GLASS BY WEIGHT.

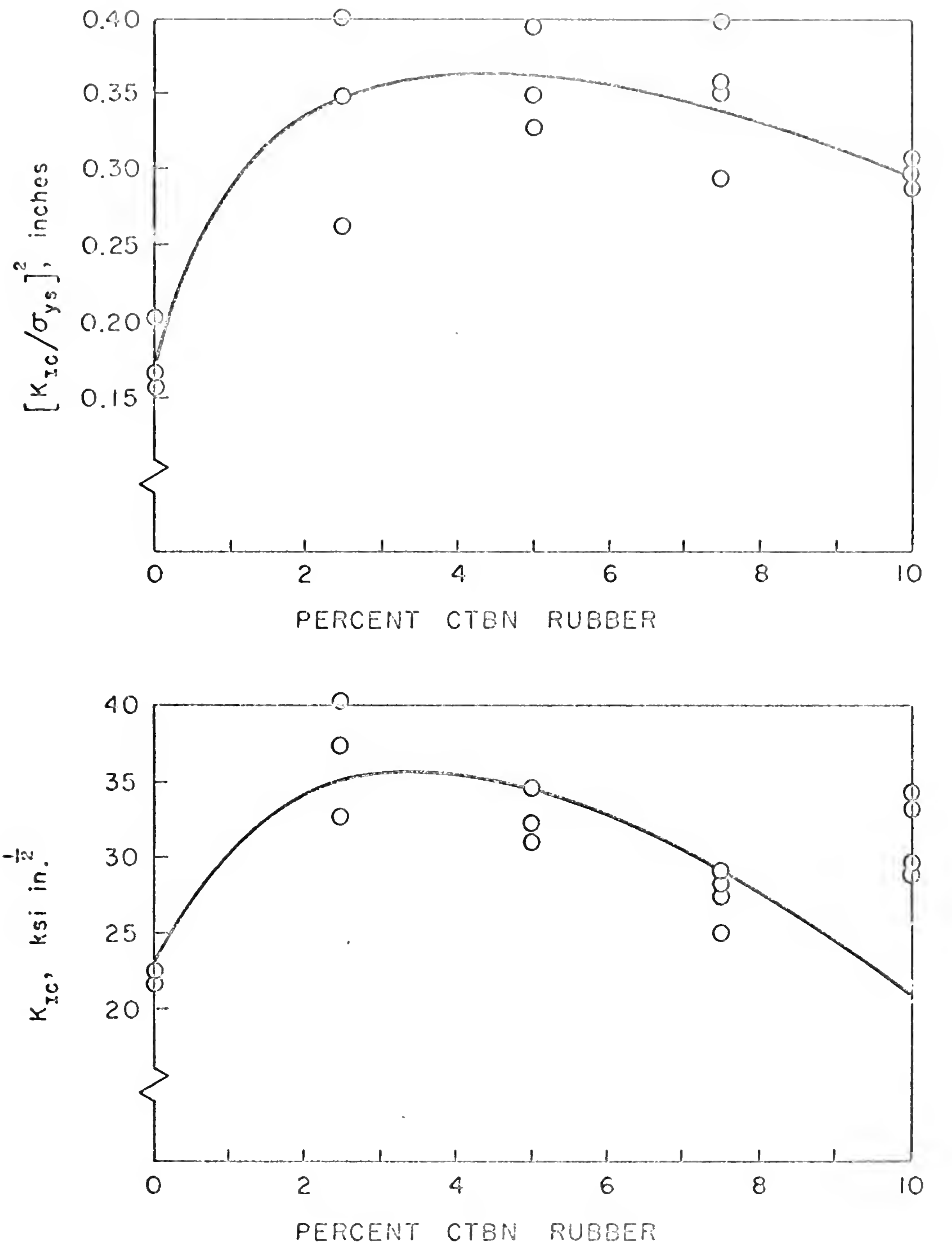

FIGURE 10. VARIATION IN $\left[K_{IC}/\sigma_{ys}\right]^2$ AND K_{IC} WITH PERCENT CTBN RUBBER.

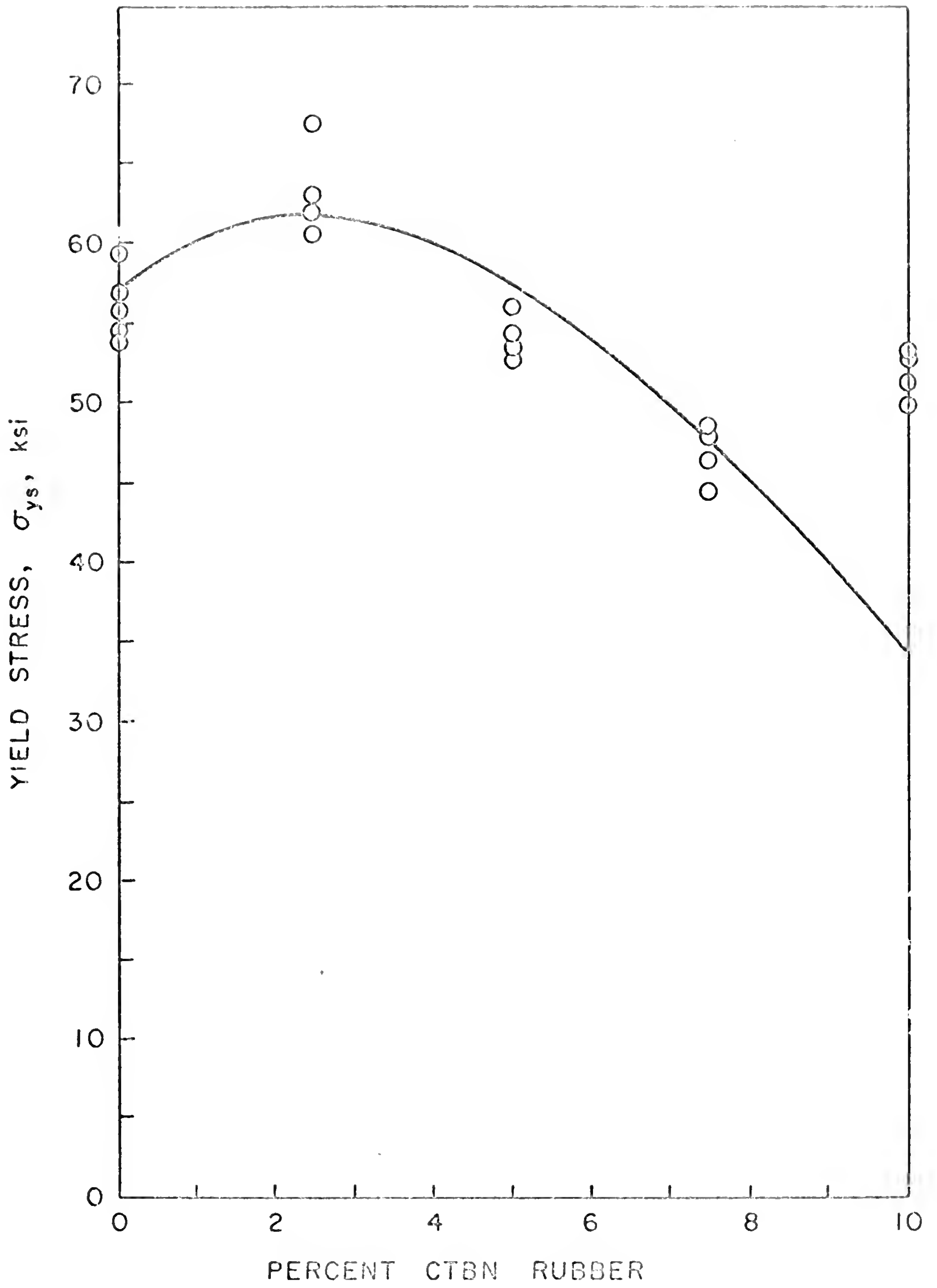

FIGURE 10a. VARIATION IN YIELD STRESS WITH PERCENT CTBN RUBBER.

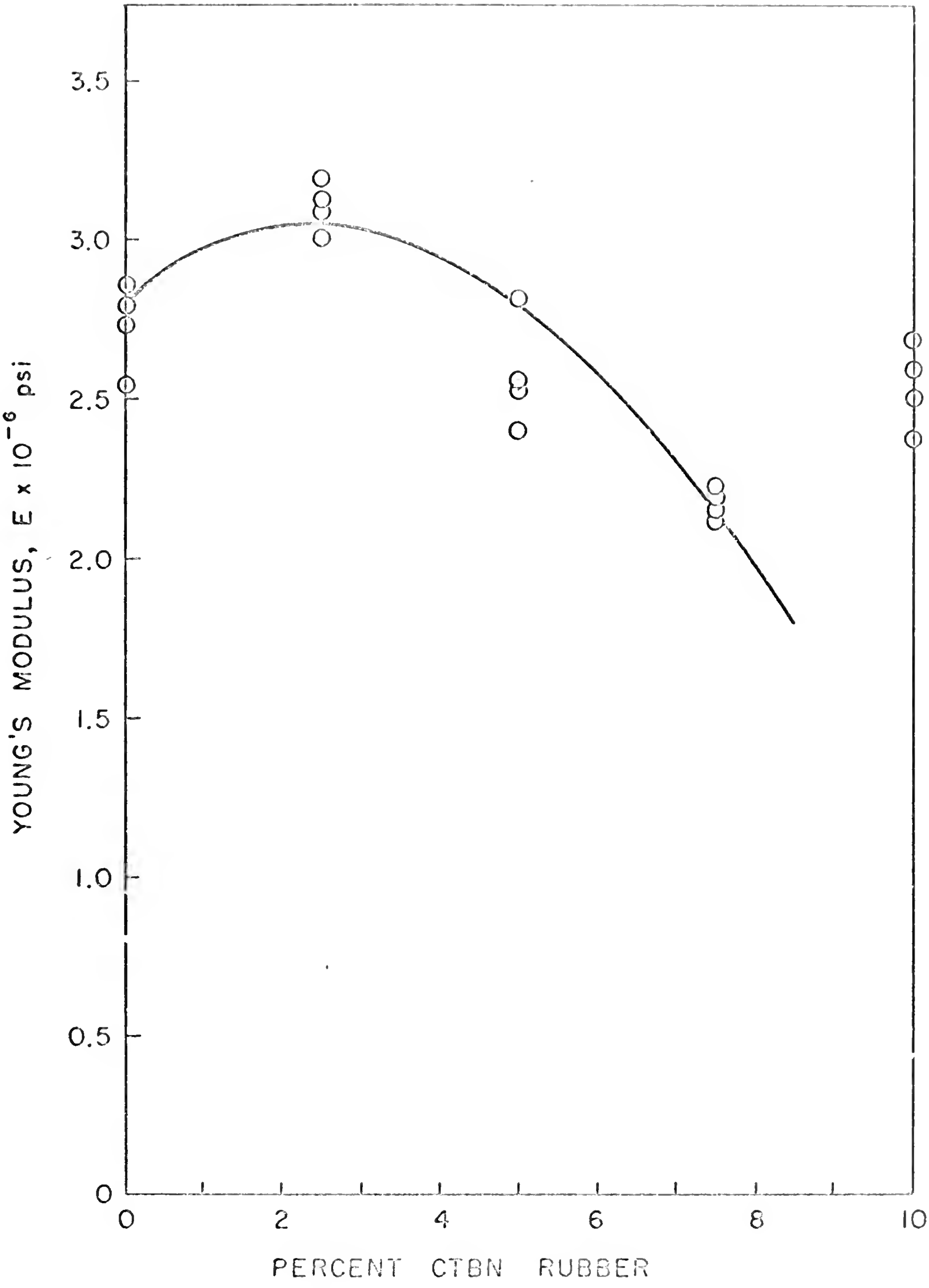

FIGURE 10b. VARIATION IN YOUNG'S MODULUS WITH PERCENT CTBN RUBBER.

TABLE 1

PROPERTIES OF LAMINAC 4173

Type	Rigid, Promoted, "Air Dry"
Viscosity	Low, slightly Thixotropic
Reactivity	High
Monomer	Styrene
Specific Gravity	1.03
Barcol Hardness	48 - 50
Tensile Strength	8,3000 psi

PROPERTIES OF STYLE 181 FIBERGLASS FABRIC

Thickness	0.0085"
Count	57 x 54
Tensile Strength, pounds per inch	340 x 330
Weave	8 H Satin
Weight, oz. sq. yd.	8.90

TABLE 2

TENSILE TEST DATA

Specimen	Area	Force	Scope x 10^{-4}	σ_{ys} x 10^{-3}	E x 10^{-6}
1-0-1	.126	1090	5.67	8.640	.45
1-0-2	.127	950	5.51	7.480	.433
1-3-1	.0215	650	--	30.2	1.39
1-3-2	.0235	700	--	24.8	1.38
1-6-1	.0313	1365	6.50	43.700	2.05
1-6-2	.0290	1390	6.34	42.900	2.18
1-6-3	.0258	1340	7.18	52.000	2.77
1-6-4	.0296	1245	6.34	42.100	2.14
2-6-1	.0222	1360	6.00	61.3	2.70
2-6-2	.0229	1380	7.18	60.4	3.12
2-6-3	.0250	1280	7.00	51.2	2.80
2-6-4	.0220	1325	6.52	60.2	2.95
1-9-1	.0364	2050	10.0	56.3	2.75
1-9-2	.0360	1875	9.36	52.1	2.60
1-9-3	.0374	2150	10.0	57.5	2.68
2-9-1	.0370	2000	9.57	54.1	2.59
2-9-2	.0373	2050	10.20	54.9	2.73
2-9-3	.0360	1900	9.75	52.9	2.73
2-9-4	.0355	1900	9.32	53.5	2.62
2-9-5	.0345	1725	9.57	50.1	2.77
1-12-1	.0564	2175	11.90	38.6	2.14
1-12-2	.0536	2780	13.75	51.9	2.56
1-12-3	.0530	2830	14.20	53.4	2.67
1-12-4	.0531	2810	12.80	53.0	2.44
1-12-5	.0566	2625	15.40	46.4	2.72

Specimen	Area	Force	Scope x 10^{-4}	σ_{ys} x 10^{-3}	E x 10^{-6}
1-15-1	.0616	3480	17.90	56.5	2.91
1-15-2	.0619	3680	16.98	59.5	2.75
1-15-3	.0609	3400	16.67	55.9	2.74
1-15-4	.0626	3560	17.45	56.8	2.79
1-15-5	.0705	3260	17.90	46.3	2.55
2-15-1	.0611	3500	17.05	57.3	2.79
2-15-2	.0590	3400	16.67	57.6	2.82
2-15-3	.0605	3400	17.65	56.3	2.92
2-15-4	.0606	3360	16.87	55.5	2.79
2-15-5	.0635	3630	17.20	57.2	2.72
1-18-1	.0720	3950	19.15	54.9	2.66
1-18-2	.0736	4350	23.70	59.1	3.23
1-18-3	.0728	3925	20.38	54.0	2.81
1-18-4	.0734	4140	20.80	56.5	2.83
1-18-5	.0750	4300	20.80	57.3	2.78
2-18-1	.0845	4040	19.15	47.8	2.24
2-18-2	.0826	4030	19.15	48.8	2.32
2-18-3	.0858	4150	20.95	48.4	2.45
2-18-4	.0815	4410	20.10	53.2	2.48
2-18-5	.0841	4390	19.15	52.1	2.28
2-18-6	.0845	4460	20.30	52.8	2.41
4-18-1	.0591	3600	18.72	60.6	3.18
4-18-2	.0604	3600	18.72	59.7	3.12
5-18-1	.1290	4600	18.72	35.2	1.46
5-18-2	.1295	4300	18.72	34.4	1.45
5-18-3	.1280	4500	20.00	35.2	1.55
6-18-1	.138	4025	17.90	29.2	1.29
6-18-2	.132	4000	16.67	30.3	1.26
6-18-3	.136	3800	17.88	28.0	1.32
6-18-4	.140	3850	21.60	27.6	1.55

Specimen	Area	Force	Scope x 10^{-4}	σ_{ys} x 10^{-3}	E x 10^{-6}
1-24-1	.0838	3900	21.60	46.5	2.59
1-24-2	.1110	5920	26.60	53.3	2.40
1-2413	.1080	5950	26.60	55.1	2.47
1-24-4	.0895	5300	26.60	59.3	2.98
1-24-5	.1100	5750	26.60	52.0	2.40
1-12-1	.0564	2175	11.90	38.6	2.14
1-12-2	.0536	2780	13.75	51.9	2.56
1-12-3	.0530	2830	14.20	53.4	2.67
1-12-4	.0531	2810	12.80	53.0	2.44
1-12-5	.0566	2625	15.40	46.4	2.72
1-15-1	.0616	3480	17.91	56.5	2.91
1-15-2	.0619	3680	16.98	59.5	2.75
1-15-3	.0609	3400	16.67	55.9	2.74
1-15-4	.0625	3560	17.45	56.8	2.79
1-15-5	.0705	3260	17.90	46.3	2.55
2-15-1	.0611	3500	17.05	57.3	2.79
2-15-2	.0590	3400	16.67	57.6	2.82
2-15-3	.0605	3400	17.65	56.3	2.92
2-15-4	.0606	3360	16.87	55.5	2.79
2-15-5	.0635	3630	17.20	57.2	2.72
1-18-1	.0720	3950	19.15	54.9	2.66
1-18-2	.0736	4350	23.70	59.1	3.23
1-18-3	.0728	3950	20.38	54.0	2.81
1-18-4	.0734	4140	20.80	56.5	2.83
1-18-5	.0750	4300	20.80	57.3	2.78
2-24-1	.104	5400	25.80	52.0	2.49
2-24-2	.103	5150	26.60	50.0	2.59
2-24-3	.104	6200	26.25	59.6	2.52
2-24-4	.101	4700	23.30	46.5	2.31
2-24-5	.101	4825	23.30	48.2	2.31
2-24-6	.101	5775	25.30	57.2	2.51

Specimen	Area	Force	Scope x 10^{-4}	σ_{ys} x 10^{-3}	E x 10^{-6}
1-30-1	.113	7600	41.70	67.2	3.69
1-30-2	.114	6150	33.35	54.0	2.92
1-30-3	.120	6875	34.20	57.0	2.85
1-30-4	.117	6800	31.60	58.1	2.72
1-30-5	.115	6350	33.35	55.2	2.89
2-30-1	.105	6000	32.80	57.2	3.12
2-30-2	.109	6000	33.35	55.0	3.06
2-30-3	.129	7250	33.35	56.2	2.58
2-30-4	.133	6907	33.35	51.9	2.51
1-48-1	.327	--	10.00	--	3.30
1-48-2	.341	--	12.40	--	3.30
1-48-3	.341	--	12.40	--	--

TABLE 3

TENSILE TESTS DATA (RUBBER MODIFIED)

% Rubber	Specimen	Area	Force	Scope x 10^{-4}	σ_{ys} x 10^{-3}	E x 10^{-6}
2.5	1	.0553	3350	16.67	60.6	3.01
	2	.0531	3350	16.67	63.0	3.13
	3	.0508	3150	16.30	62.0	3.20
	4	.0505	3400	15.85	67.4	3.14
5.0	1	.0620	3325	17.50	53.6	2.82
	2	.0625	3500	17.50	56.0	2.53
	3	.0626	3400	15.85	54.3	2.53
	4	.0652	3450	15.85	53.0	2.43
7.5	1	.0754	3600	16.67	47.8	2.21
	2	.0748	3450	16.30	46.2	2.17
	3	.0770	3400	17.10	44.2	2.22
	4	.0774	3715	16.67	47.9	2.16
10.0	1	.0617	3300	16.67	53.4	2.70
	2	.0604	3300	15.85	54.6	2.62
	3	.0634	3350	15.85	53.0	2.50
	4	.0664	3325	15.85	50.0	2.38

TABLE 4

EFFECT OF NOTCH DEPTH ON K_{1c} AND $[K_{1c}/\sigma_{ys}]^2$

Specimen	Notch Depth	σ_{ys}	K_{1c}	$[K_{1c}/\sigma_{ys}]^2$
1-12-1	0.300	51,200	24.6	0.230
1-12-2	0.286	51,200	24.7	0.232
1-12-3	0.322	51,200	27.0	0.274
1-12-5	0.203	51,200	31.6	0.375
2-12-1	0.450	52,000	24.0	0.213
2-12-2	0.600	52,000	23.0	0.196
2-12-3	0.900	52,000	22.6	0.189
2-12-4	0.300	52,000	24.8	0.226
2-12-5	0.300	52,000	24.2	0.214
1-48-1	0.400	55,000	22.8	0.170
1-48-3	0.300	55,000	21.4	0.152
1-48-5	0.250	55,000	22.5	0.166
1-48-6	0.500	55,000	23.1	0.176
1-48-7	0.250	55,000	20.5	0.140
1-48-9	0.135	55,000	22.1	0.162

TABLE 5

EFFECT OF THICKNESS ON K_{1c} AND $[K_{1c}/\sigma_{ys}]^2$

Specimen	σ_{ys}	K_{1c}	$[K_{1c}/\sigma_{ys}]^2$
1-3-1	30,200	19.1	.405
1-3-2	30,200	20.6	.457
1-3-3	30,200	18.1	.358
1-3-4	30,200	17.6	.340
1-6-1	44,200	17.9	.164
1-6-2	44,200	22.7	.253
1-6-3	44,200	21.4	.234
1-9-1	55,200	25.1	.205
1-9-2	55,200	23.6	.183
1-9-3	55,200	23.0	.173
2-9-1	53,100	29.4	.306
2-9-2	53,100	23.0	.288
1-12-1	51,200	24.6	.230
1-12-2	51,200	24.1	.233
1-12-3	51,200	27.0	.275
1-15-5	57,200	22.2	.151
2-15-1	56,800	26.9	.224
2-15-4	56,800	23.1	.166
1-18-2	56,400	24.8	.196
1-18-4	56,400	26.2	.214
2-18-2	50,500	--	--
2-18-4	50,500	20.4	.161
2-18-5	50,500	22.7	.192
1-24-4	53,400	21.6	.164
1-24-5	53,400	25.0	.218
2-24-4	50,800	23.3	.211

Specimen	σ_{ys}	K_{1c}	$[K_{1c}/\sigma_{ys}]^2$
1-30-5	56,150	22.8	.163
2-30-4	54,100	26.8	.244
2-30-5	54,100	26.0	.232
1-48-1	55,000	22.8	.172
1-48-3	55,000	21.4	.152
1-48-4	55,000	20.6	.140
1-48-5	55,000	22.5	.167
1-48-6	55,000	23.1	.175
1-48-7	55,000	20.5	.140

TABLE 6

EFFECT OF CROSSHEAD SPEED ON K_{1c} AND $[K_{1c}/\sigma_{ys}]^2$

Specimens tested with approximately 70% glass

Specimen	Crosshead Rate (in/min)	σ_{ys}	K_{1c}	$[K_{1c}/\sigma_{ys}]^2$
1-15-1	0.002	55,000	24.6	.200
1-18-1	0.002	56,300	27.8	.244
1-24-1	0.005	53,400	25.0	.219
2-24-1	0.005	50,800	27.2	.276
1-15-2	0.020	55,000	27.0	.240
2-18-1	0.020	50,500	25.6	.256
1-24-4	0.050	53,400	21.6	.164
1-24-5	0.050	53,400	25.0	.218
2-24-4	0.050	50,800	23.3	.211
1-15-5	0.050	55,000	22.2	.163
2-15-4	0.050	56,800	23.1	.166
2-18-4	0.050	50,500	22.7	.202
1-24-2	0.500	53,400	29.5	.305
2-24-3	0.500	50,800	30.0	.347
1-24-2	5.000	53,400	32.9	.380
2-24-3	5.000	50,800	33.3	.427
1-18-3	20.000	56,300	40.8	.527
2-15-3	20.000	56,800	36.9	.420
6-18-1	0.050	28,900	14.9	.264
6-18-2	0.050	28,900	16.4	.321
6-18-4	0.010	28,900	15.8	.297
6-18-5	0.100	28,900	17.0	.346
6-18-6	1.000	28,900	18.3	.400
6-18-7	10.000	28,900	19.8	.470
6-18-8	1.000	28,900	17.8	.379

TABLE 7

EFFECT OF GLASS CONTENT ON K_{1c} AND $[K_{1c}/\sigma_{ys}]^2$

Specimen	σ_{ys}	E	K_{1c}	$[K_{1c}/\sigma_{ys}]^2$	% Glass
1-18-2	56,300	2.80	24.8	.194	74.5
1-18-4	56,300	2.80	26.2	.215	74.5
2-18-4	50,500	2.36	20.4	.162	69.0
2-18-5	50,500	2.36	22.7	.200	69.0
3-18-2	56,100	2.55	37.2	.436	77.9
3-18-3	56,100	2.55	38.1	.460	77.9
4-18-1	60,200	3.15	40.1	.443	83.6
4-18-2	60,200	3.15	41.7	.477	83.6
4-18-3	60,200	3.15	39.2	.422	83.6
5-18-1	34,900	1.50	16.5	.223	50.5
5-18-2	34,900	1.50	15.8	.204	50.5
5-18-3	34,900	1.50	18.0	.264	50.5
5-18-4	34,900	1.50	18.1	.266	50.5
5-18-5	34,900	1.50	18.7	.285	50.5
6-18-1	28,900	1.36	14.9	.267	41.5
6-18-2	28,900	1.36	16.4	.330	41.5
6-18-3	28,900	1.36	14.6	.254	41.5

TABLE 8

PROPERTIES OF LAMINATES

Laminate	Layers of Cloth	$\overline{\sigma}_{ys}$	$\overline{E} \times 10^{-6}$	% Glass
1-3	3	30,000	1.38	50.0
1-6	6	44,000	2.15	69.4
1-9	9	55,200	2.65	76.8
2-9	9	53,100	2.70	71.4
1-12	12	51,200	2.50	72.6
1-15	15	55,000	2.75	69.6
2-15	15	56,800	2.80	72.7
1-18	18	56,300	2.80	74.5
2-18	18	50,500	2.36	69.0
3-18	18	56,100	2.55	77.9
4-18	18	60,200	3.15	83.6
5-18	18	34,900	1.50	50.5
6-18	18	28,900	1.36	41.5
1-24	24	53,400	2.43	74.0
2-24	24	50,800	2 40	71.3
1-30	30	56,150	2.81	77.0
2-30	30	54,100	2.55	70.1
1-48	48	55,000	3.30	69.2
1-0	0	8,060	.45	0

TABLE 9

RUBBER EFFECT

	σ_{ys}	K_{1c}	$[K_{1c}/\sigma_{ys}]^2$
2.5-1	63,200	32.8	.268
-2	63,200	37.5	.350
-3	63,200	40.7	.412
5.0-2	54,200	32.2	.352
-3	54,200	31.0	.327
-4	54,200	34.6	.395
7.5-1	46,500	28.1	.367
-2	46,500	25.2	.294
-3	46,500	27.8	.352
-4	46,500	29.6	.404
10.0-1	52,700	29.0	.315
-2	52,700	33.2	.295
-3	52,700	28.9	.300
-4	52,700	34.8	.435

TABLE 10

EFFECT OF CTBN RUBBER ON SURFACE WORK

% Rubber	K_{1c}, $KSI \cdot (in)^{\frac{1}{2}}$	ΔK_{1c}	$E \times 10^{-6}$	ΔE	$\frac{\Delta\gamma}{\gamma}$
0	24.1	--	2.75	--	0
2.5	37.0	12.9	3.12	0.37	0.825
5.0	33.3	9.2	2.58	-0.17	0.804
7.5	27.7	3.6	2.19	-0.56	0.502
10.0	31.5	7.4	2.57	-0.18	0.712

12